JGR Biogeosciences

RESEARCH ARTICLE
10.1029/2020JG005804

**Key Points:**
- During storms, the carbon species entering the stream change reflecting shifts in the terrestrial flowpaths contributing to streamflow
- Percent new water was related to carbon concentration and form providing a clear link between stream sources and soil carbon source pools
- Ultrahigh-resolution mass spectrometry showed stream DOM molecular properties draining the upland forest converging on those of the wetlands

**Supporting Information:**
- Supporting Information S1

**Correspondence to:**
J. B. Fellman,
jbfellman@alaska.edu

**Citation:**
Fellman, J. B., Hood, E., Behnke, M. I., Welker, J. M., & Spencer, R. G. M. (2020). Stormflows drive stream carbon concentration, speciation, and dissolved organic matter composition in coastal temperate rainforest watersheds. *Journal of Geophysical Research: Biogeosciences*, *125*, e2020JG005804. https://doi.org/10.1029/2020JG005804

Received 23 APR 2020
Accepted 25 AUG 2020
Accepted article online 9 SEP 2020



# Stormflows Drive Stream Carbon Concentration, Speciation, and Dissolved Organic Matter Composition in Coastal Temperate Rainforest Watersheds

**Jason B. Fellman[1], Eran Hood[1], Megan I. Behnke[2], Jeffrey M. Welker[3,4], and Robert G. M. Spencer[2]**

[1]Department of Natural Sciences and Alaska Coastal Rainforest Center, University of Alaska Southeast, Juneau, AK, USA, [2]Department of Earth, Ocean, and Atmospheric Science, Florida State University, Tallahassee, FL, USA, [3]Department of Biological Sciences, University of Alaska Anchorage, Anchorage, AK, USA, [4]Department of Ecology and Genetics, University of Oulu & UArctic, Oulu, Finland

**Abstract** Stream water carbon concentrations can be highly dynamic on the time scales of both individual storm events and seasonal hydroclimatic shifts. We collected stream water daily over a 6-day storm from three headwater subcatchments of varying landcover (poor fen, forested wetland, and upland forest) and the catchment outlet to evaluate how precipitation events impact the concentration and speciation of carbon (organic vs. inorganic) as well as the composition of dissolved organic matter (DOM) exported laterally from coastal temperate rainforest catchments. Dissolved and particulate organic carbon concentrations increased during the storm at all sites, while dissolved inorganic carbon concentrations were diluted during peak flows. These results highlight the importance of quantifying all forms of lateral carbon export when evaluating the role of storms in catchment-scale carbon cycling. Isotopic hydrograph separation using stream water $\delta^{18}O$ showed that percent new water was significantly related to carbon concentration and form providing a clear link between stream water sources (i.e., recent event water) and soil carbon source areas that become connected to surface water during storms. Furthermore, ultrahigh-resolution mass spectrometry showed that stream water DOM exported from the upland forest contained the greatest molecular diversity of the three landscape types and had the largest changes in composition over the storm suggesting that the wetland-dominated subcatchments were less compositionally diverse with regard to soil DOM pools active during the storm. Overall, this study provides insight into hydro-biogeochemical drivers that control lateral carbon export from forested catchments in a region where an increasing fraction of precipitation is falling as rain.

**Plain Language Summary** Streams transport large amounts of terrestrially derived carbon to the ocean, especially during large rainstorms. We collected water samples daily over a 6-day storm from small drainage areas of varying landcover to see how the concentration and type of carbon changed over the course of a storm. Our results show that the amount and type of carbon in the stream changed dramatically during the storm and originated from different areas of the landscape. The flow of water through the soil also changed during the storm and was related to the type and amount of carbon entering the stream. Storm events not only impact carbon entering the stream but also may impact its transfer to coastal marine ecosystems. Climate in the study region is projected to become warmer and wetter in coming decades. These shifts in climate could lead to more carbon export during storms, especially during winter because of more precipitation falling as rain rather than snow.

## 1. Introduction

Riverine transport of carbon (C), as dissolved inorganic (DIC), dissolved organic C (DOC), and particulate organic C (POC), is increasingly recognized as contributing to the global C cycle (Battin et al., 2009; Cole et al., 2007; Drake et al., 2017; Tranvik et al., 2009). As a result, the quantification of C movement across the land-water interface, which is estimated at $>5.0$ Pg $yr^{-1}$ globally (Butman et al., 2018; Drake et al., 2017), and how the speciation of this flux varies across ecosystem types are essential topics of study within the aquatic and Earth sciences (Csank et al., 2019; Tomco et al., 2019). Previous studies in small forested catchments

show that rainfall-runoff processes are key drivers of the lateral export of terrestrial C to surface waters (Boyer et al., 1997; Hinton et al., 1997; Raymond & Saiers, 2010; Vaughan et al., 2019), with the bulk of annual catchment DOC export typically occurring during high flow events (Raymond et al., 2016; Wiegner et al., 2009; Wilson et al., 2013). However, we still lack a fundamental understanding of how multiple forms of C (including DOC, POC, and DIC) simultaneously vary during high flow events (Tank et al., 2018), which is critical to understanding the role of storm-driven lateral C export in the overall catchment C cycle.

Event-driven shifts in lateral C export are often coupled with changes in dissolved organic matter (DOM) chemical composition (Fellman et al., 2009; Hood et al., 2006) and biolability (Wiegner et al., 2009; Wilson et al., 2013) because DOM source pools mobilized during high flows differ from those that are hydrologically linked to surface water during baseflow. The use of Fourier-transform ion cyclotron resonance mass spectrometry (FT-ICR MS) to characterize stream water DOM has flourished in the last decade because it yields a precise molecular fingerprint of the DOM pool that includes information on elemental ratios and compound classes (Spencer et al., 2015; Stubbins et al., 2014; Wagner et al., 2019). High-resolution sampling of streams draining forested watersheds recently illustrated that FT-ICR MS can trace molecular-level hysteresis patterns in the DOM pool during stormflows (Wagner et al., 2019), information that can help elucidate the potential fate of pulsed DOM delivery to downstream ecosystems, including nearshore marine environments.

At the catchment scale, evaluating the relationship between stream water C export and discharge across a range of hydrological conditions can elucidate whether lateral C export and speciation is controlled by C production in the terrestrial ecosystem or by hydrologic connectivity between C source pools and surface waters (Moatar et al., 2017; Pellerin et al., 2012; Vaughan et al., 2019; Zarnetske et al., 2018). For example, an increase in DOC concentration during stormflows suggests that extensive soil source pools of DOC exist, but a lack of watershed hydrologic connectivity limits the transport of this DOC across the terrestrial-aquatic interface. Thus, combining C concentration and speciation data with catchment hydrologic tracers that provide information about streamflow generation, such as stable isotopes of water ($\delta^{18}O$ and $\delta^{2}H$; Benettin et al., 2015; Kirchner, 2016; Stockinger et al., 2016; Tomco et al., 2019), allows for a more nuanced understanding of how different forms of C are transported laterally to surface waters.

The Pacific coastal temperate rainforest (PCTR) contains some of the densest C stocks in the world (>500 Mg C $ha^{-1}$; McNicol et al., 2019) and extremely high rates of specific discharge (1.5–6 m $yr^{-1}$; Neal et al., 2010). However, there have been few catchment-scale studies of C speciation and export from this biome (Argerich et al., 2016), particularly in comparison to other northern high-latitude biomes such as boreal forests and permafrost-dominated Arctic watersheds (Holmes et al., 2012; Laudon et al., 2004; Raymond et al., 2007; Striegl et al., 2007). Here, we combine measurements of stream water $\delta^{18}O$ and FT-ICR MS analyses of DOM with concentrations of DOC, DIC, and POC to evaluate how stormflows drive the form of C and molecular fingerprint of DOM exported laterally from a forested catchment in the PCTR. We hypothesized that recent event water, as determined from isotopic hydrograph separation of stream water $\delta^{18}O$, varied with the concentration and form of C and molecular properties of DOM exported during the storm. Stream water was collected at least daily over a 6-day storm from three of the most common landcover types in the region (poor fen, forested wetland, and upland forest; D'Amore et al., 2015) and the catchment outlet stream. This design allowed us to examine how the biogeochemical signature at the catchment outlet is controlled by inputs of DOM from streams draining the three landcover types at various points of the storm hydrograph.

## 2. Methods

### 2.1. Site Description

Stream water was collected from three tributary streams draining subcatchments and at outlet of the Fish Creek catchment near Juneau, AK, in the northern region of the PCTR (Figure 1). The Juneau area has a moderate maritime climate (i.e., cool summers and mild winters) with abundant precipitation (2,000 mm at sea level) that generally falls during large frontal storms that form in the northern Pacific Ocean and move eastward into southeast Alaska and western Canada (D'Amore et al., 2015). The Fish Creek catchment (area of 36 $km^2$ and mean elevation of 487 m) contains intrusive volcanic and sedimentary rock in the Stephens

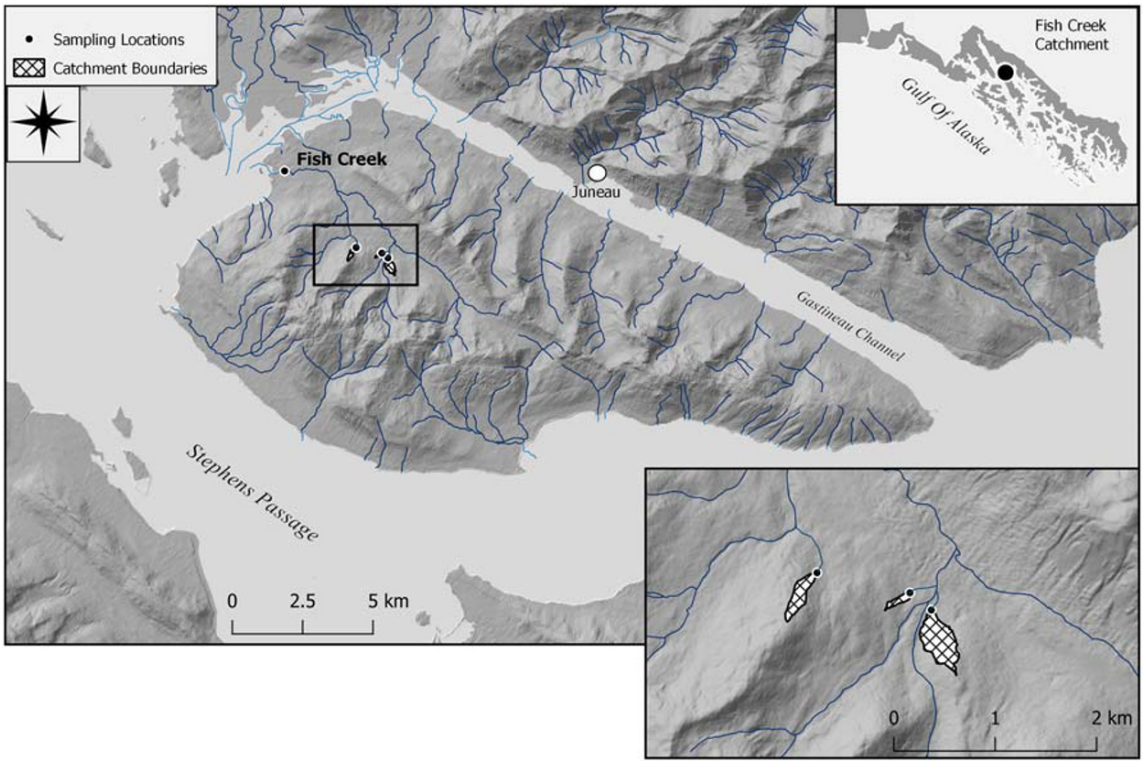


**Figure 1.** Map of the study catchment and sampling locations near Juneau, Alaska.

Passage volcanic subsection (D'Amore et al., 2015). The catchment is a mix of physiographic features including productive temperate rainforest, wetlands, and high elevation alpine areas that contain snow through much of the summer.

The three subcatchments we sampled are characterized by distinct landcover types that vary across a soil drainage gradient common to the PCTR. The poor fen is typical of the poorly drained slope bog wetland type (National Wetlands Working Group [NWWG], 1988) with acidic soils (pH 4), peat accumulations >2 m deep, and vegetation consisting of *Sphagnum* mosses (*Sphagnum* spp.), ericaceous shrubs, sedges, and shore pine (*Pinus contorta* var. *contorta*) (Fellman et al., 2008). The forested wetland is typical of the raised peatland swamp (NWWG, 1988), with acidic soils (pH 4.0) and 0.50- to 0.75-m-deep peat overlaying glacial till (Fellman et al., 2008). Forested wetland vegetation consists of *Sphagnum* mosses (*Sphagnum* spp.), skunk cabbage (*Lysichiton americanum*), and blueberry (*Vaccinium* spp.) with an overstory of mainly western hemlock (*Tsuga heterophylla*) and Sitka spruce (*Picea sitchensis*). Although the forested wetland and poor fen formed on the same deposit, the sites maintain different hydrologic regimes where soil hydraulic conductivity is greater in the forested wetland but soil saturation is sufficient to support anoxic conditions (D'Amore et al., 2010). Soils in the upland forest are Spodosols (Typic Humicryod) that are acidic (pH 4.0), moderately deep, and moderately well drained, due to the steep slopes (Fellman et al., 2008). Upland forest vegetation consists of blueberry (*Vaccinium* spp.) with an overstory of mainly western hemlock and Sitka spruce.

### 2.2. Stream Water Collection and Analyses

Surface water grab samples were collected at least daily (samples were collected twice on 9 August) over the course of a 6-day storm event in August 2018 from the three subcatchments and the Fish Creek outlet. Higher-resolution sampling (collecting stream water multiple times over multiple days) was not feasible for this study due to remote site access. Water temperature, specific conductivity, and pH were measured using a hand-held YSI (Professional Plus) unit. Stream water for DOC (collected in duplicate) and FT-ICR MS analysis was field filtered through precombusted (>4 hr at 450°C) Whatman GF/F filters (0.7-μm pore size). Samples for DOC were stored in precombusted (>4 hr at 550°C) amber glass vials and refrigerated until analyzed within 48 hr of collection while DOM for FT-ICR MS measurement was stored in acid-washed

polycarbonate (PC) bottles and frozen until solid-phase extraction. Concentrations of DOC were determined via nonpurgeable organic C analysis on a Shimadzu TOC-LC/TN analyzer. Analytical precision (mean standard deviation for reanalysis of identical samples) for DOC was 0.1 mg C $L^{-1}$ for samples less than 10 and 0.3 mg C $L^{-1}$ for samples greater than 20 mg C $L^{-1}$. Samples were acidified and sparged to remove inorganic C followed by high-temperature combustion and analysis on the TOC analyzer (Stubbins & Dittmar, 2012).

Samples for POC were collected in 2-L PC bottles by collecting a water sample across the depth of the stream channel. Upon returning to laboratory, a known volume of water (between 1 and 2 L) was filtered through a precombusted (>4 hr at 450°C) Whatman GF/F filter followed by drying at 40°C and reweighing to calculate a sediment concentration. Filters were acidified to remove carbonates by a repeated sulfurous acid addition (Connelly et al., 2015) and packed in tin capsules for C analysis on a LECO CHN analyzer. Concentrations of POC (mg $L^{-1}$) were determined by dividing the elemental C concentration by the known volume of water that passed through the filter.

Concentrations and speciation of DIC were determined by measurements of dissolved $CO_2$ and alkalinity. Triplicate samples of dissolved $CO_2$ were collected in 60-ml syringes using a headspace equilibration where the headspace was initially purged with helium followed by shaking for 1 min. Collected gas was injected into pre-evacuated 20-ml vials followed by analysis the same day on a LI-COR (LI-7000 $CO_2/H_2O$) infrared gas analyzer. Concentrations of $CO_2$ (mg C $L^{-1}$) were determined using standard calculations that included air and water temperature (measured with a hand-held YSI), elevation, and atmospheric pressure (Worrall et al., 2005), which were obtained from a National Weather Service weather station (Juneau airport) near the mouth of Fish Creek. Unfiltered stream water samples were measured for alkalinity as $CaCO_3$ (mg $L^{-1}$) in the laboratory by titration to two pH end points (pH 4.7 and 4.4) using 0.02-N hydrochloric acid. Carbonate alkalinity was converted to bicarbonate ($HCO_3^-$) concentration, which was used to calculate total DIC in mg C $L^{-1}$ ($HCO_3^- + CO_2$).

Water isotope samples were collected in glass bottles with zero headspace and stored at room temperature until analysis on a Picarro L2120-*i* analyzer (analytical precision of 0.05‰). Isotope values for $\delta^{18}O$ are reported in per mil (‰) after normalization to Vienna standard mean ocean water (VSMOW). Discharge in Fish Creek was measured at 15-min intervals using a stilling well that contained a pressure transducer (In-Situ Level TROLL). Discharge measurements ($n = 20$) using a SonTek FlowTracker ADV were completed across a wide range of flow conditions over the summer of 2018, and the stage-discharge relationship was used to calculate streamflow. Additionally, stilling wells were used to record stage in the three subcatchment outlet streams using pressure transducers (Hobo model U20) that measured water height every 30 min. We were not able to quantify discharge in the three subcatchments due to an insufficient number of flow measurements needed to build stage-discharge relationships at each site.

### 2.3. Fourier-Transform Ion Cyclotron Resonance Mass Spectrometry

Samples for FT-ICR MS analysis were solid-phase extracted onto reversed phase Bond Elut Priority PolLutant (PPL) columns (100 mg; Agilent) following Dittmar et al. (2008). Acidified (pH 2) samples were passed through precleaned PPL columns with volumes adjusted to a target concentration of 40 μg C $ml^{-1}$ in methanol (JT Baker HPLC grade) elutes. Extracted samples were stored at −20°C until analysis on a 21-T FT-ICR MS at the National High Magnetic Field Laboratory (Tallahassee, Florida; Hendrickson et al., 2015; Smith et al., 2018) with direct infusion negative electrospray ionization. Each mass spectrum consisted of 100 coadded time domain acquisitions.

Molecular formulae were assigned to peaks with >6$\sigma$ root-mean-square baseline noise (Koch et al., 2007; Stubbins et al., 2010) with PetroOrg ©™ software (Corilo, Yuri. PetroOrg, Florida State University, 2015). Allowed formulae had elemental bounds of $C_{1-45}H_{1-92}N_{0-4}O_{1-25}S_{0-2}$ and a mass accuracy ≤300 ppb. The modified aromaticity index ($AI_{mod}$) was calculated to assess the degree of unsaturation based on molecular formula (Koch & Dittmar, 2006, 2016). Compound classes were defined using $AI_{mod}$ and elemental ratios as follows: polyphenolics (0.5 $AI_{mod} \leq 0.66$); condensed or polycyclic aromatic ($AI_{mod} > 0.66$); highly unsaturated and phenolic (HUP) ($AI_{mod} \leq 0.5$, H/C 1.5, O/C ≤ 0.9); aliphatic (1.5 ≤ H/C ≤ 2.0, O/C ≤ 0.9, and N = 0); and sugar-like (O/C > 0.9). Though precise molecular formulae can be assigned to FT-ICR MS peaks, each peak may represent multiple isomers, and exact compound structure cannot be determined. Relative abundances of each formula were determined by normalizing individual peak magnitudes to the sum of

all assigned peaks in each sample, and all reported percentages refer to percent relative abundances unless otherwise noted. The contribution of each compound class was found as the sum of the relative abundances in each compound class divided by the summed abundance of all assigned formulae in each sample expressed as a percent. Similar calculations were used to determine the relative abundance of compounds containing different elements (e.g., CHO).

### 2.4. Data Analysis

The hysteresis index (HI) was used in Fish Creek, the only site with discharge, to measure the width of the hysteresis loop (i.e., difference in concentration on the rising compared to falling limb of the hydrograph) at the midpoint discharge of the event for concentrations of C and DOM molecular compound class relative abundances (Lawler et al., 2006). The HI was calculated according to Lawler et al. (2006) as

$$Q_{\text{mid}} = k(Q_{\text{max}} - Q_{\text{min}}) + Q_{\text{min}} \quad (1)$$

where $Q_{\text{mid}}$ is the midpoint discharge for the storm, $Q_{\text{max}}$ is the peak flow of the storm, $Q_{\text{min}}$ is the starting flow of the storm, and $k$ (set here at 0.5) is the midpoint discharge on the rising limb of the storm hydrograph. The HI is then determined for clockwise hysteresis as

$$\text{HI} = (\text{C}_{\text{RL}}/\text{C}_{\text{FL}}) - 1 \quad (2)$$

or for counterclockwise as

$$\text{HI} = (-1/(\text{C}_{\text{RL}}/\text{C}_{\text{FL}})) + 1 \quad (3)$$

where $\text{C}_{\text{RL}}$ and $\text{C}_{\text{FL}}$ are the C concentrations on the rising limb and falling limb of the storm, respectively.

A two-component isotopic hydrograph separation (Klaus & McDonnell, 2013; Shanley et al., 2002; J. B. Shanley et al., 2015) was applied to all stream sites. A three-component separation method was not possible because there was no sufficient data, such as soil water isotopic values. The new and old components of the storm hydrograph were calculated at the time of sampling using the $\delta^{18}$O value of rainfall during the storm for new water and the pre-event stream water in each stream for old water as follows:

$$\text{F}_{\text{p}} = (\text{C}_{\text{t}} - \text{C}_{\text{e}})/(\text{C}_{\text{p}} - \text{C}_{\text{e}}) \quad (4)$$

where $\text{F}_{\text{p}}$ is the fraction of pre-event water, $\text{C}_{\text{t}}$ is the $\delta^{18}$O value of streamflow, $\text{C}_{\text{p}}$ is the $\delta^{18}$O value of pre-event water, and $\text{C}_{\text{e}}$ is the $\delta^{18}$O value of event water (rainfall). We assumed that the isotopic signature of rainfall (new water) did not vary in space and time over the storm and that the pre-event water (old water) was similar to soil water throughout the catchment (Klaus & McDonnell, 2013). The uncertainty in new water over the storm hydrograph was 6.0%, calculated according to the methods of Genereux (1998).

To assess how C concentration and form as well as DOM composition changed over the storm and across sites, we performed a principal component analysis (PCA) of samples taken across the storm hydrograph in R Core Team using the factoextra package (Kassambara & Mundt, 2017). All C species concentration data, $\delta^{18}$O values, and FT-ICR MS compound class and elemental composition information were included in the PCA. Linear regression was used to assess the relationship between C concentration and stream $\delta^{18}$O for all sites together. Regression analyses were performed in SPSS software. When necessary, C concentration data were log transformed to meet the basic assumptions of regression analyses.

## 3. Results

### 3.1. Catchment Hydrology and Stable Water Isotopes

During the 6-day period of sampling, approximately 6.2 cm of rain fell in the Fish Creek catchment. This rainfall resulted in a moderate increase in stage height in the poor fen and upland forest but nearly fourfold increase in the forested wetland (Figures 2a–2c). Discharge in Fish Creek increased from a prestorm low of 0.3 $m^3\ s^{-1}$ to nearly 11.0 $m^3\ s^{-1}$ during peak flow, which is more than 5× the mean daily discharge (2.1 $m^3\ s^{-1}$) for Fish Creek for the period of May through October (Supporting Information Figure S1). Two precipitation samples collected from the Fish Creek catchment during the storm had a mean $\delta^{18}$O

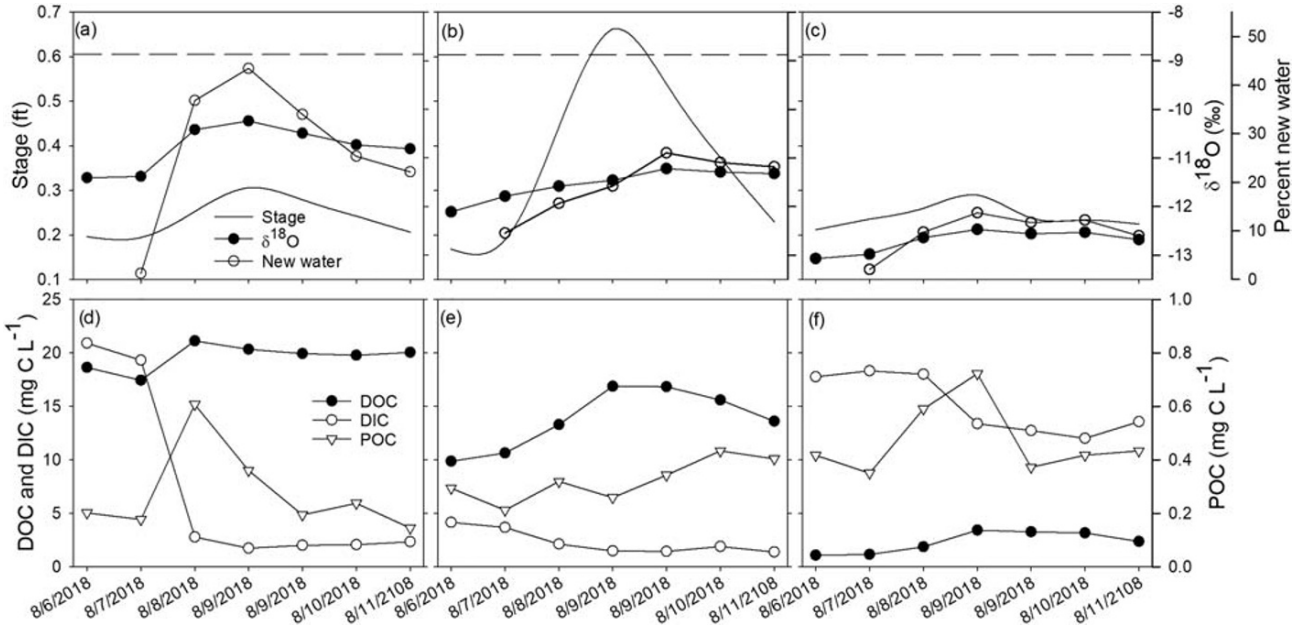


**Figure 2.** Relationship between (a–c) stage, stream water $\delta^{18}O$ values (right *y* axis), and percent new water (right offset *y* axis) and (d–f) concentrations of DOC, DIC, and POC for the poor fen (a, d), forested wetland (b, e), and upland forest (c, f) over the storm (stream water was collected twice on 9 August). The average $\delta^{18}O$ value (−8.7‰) for two rainfall samples collected throughout the storm is shown in panels (a)–(c) as a short dashed line.

value of −8.7‰ (Figure 2). In the three tributary streams, $\delta^{18}O$ values increased with flow and became more similar to rainfall, reflecting an increased contribution of recent event water to streamflow (Figures 2a–2c; Supporting Information Table S1). Isotopic hydrograph separation showed that the highest contribution of new water occurred during peak flow in all tributaries, with new water contributing to as much as 43% of streamflow in the poor fen, but less so in the forested wetland (26%) and upland forest (14%) (Figures 2a–2c). New water generally contributed more to streamflow on the descending limb of the storm hydrograph compared to the ascending limb in all three tributaries. In the Fish Creek mainstem, $\delta^{18}O$ values showed a counterclockwise hysteresis indicating that water entering the stream later in the storm was more enriched and similar to rainfall compared to water early in the storm (Figure 3a). New water contributed to 5–37% of streamflow in Fish Creek during the storm, with the highest contribution of new water occurring during peak flow (Supporting Information Figure S1).

### 3.2. Hydrologically Driven Shifts in Stream Water C Concentrations and Form

Prestorm DOC concentrations in tributary streams were 1.1 to 18.7 mg C $L^{-1}$ with the highest concentrations in the poor fen (Figures 2d–2f; Supporting Information Table S1). Concentrations of DOC increased by 2.4–7.0 mg C $L^{-1}$ in the tributary streams during the storm, which resulted in a proportional DOC increase of more than 300% in the upland forest but less than 100% in the two wetland sites. Stream water DOC concentrations in the poor fen remained above 20 mg C $L^{-1}$ and close to their peak value of 21.1 mg C $L^{-1}$ even as flow receded. In the Fish Creek mainstem, DOC showed a counterclockwise hysteresis (HI = −0.78) with lower concentrations on the ascending limb of the storm hydrograph relative to the descending limb suggesting that the hydrologic connection with DOC-rich wetland waters continued to increase after the stormflow peak (Figure 3b). For all sites together, DOC concentrations were positively related to percent new water across the storm hydrograph ($r^2 = 0.40$, $p$ 0.001, Figure 4a).

Stream water POC concentrations in all three tributaries were much lower (0.5 to 1.4 mg C $L^{-1}$) and varied less with flow relative to DOC, except in the poor fen where concentrations more than doubled during the storm (Figures 2d–2f). As a result, ratios of DOC to POC in the poor fen decreased with increasing storm discharge, and the coefficient of variation (CV) was greater for POC (0.59) than DOC (0.06) over the storm. In the forested wetland and upland forest, DOC:POC increased with flow during the storm. Concentrations of POC in Fish Creek showed a mild clockwise hysteresis (HI = 0.15), although concentrations were quite variable on the falling limb relative to the ascending limb of the storm hydrograph (Figure 3c). Similar to the

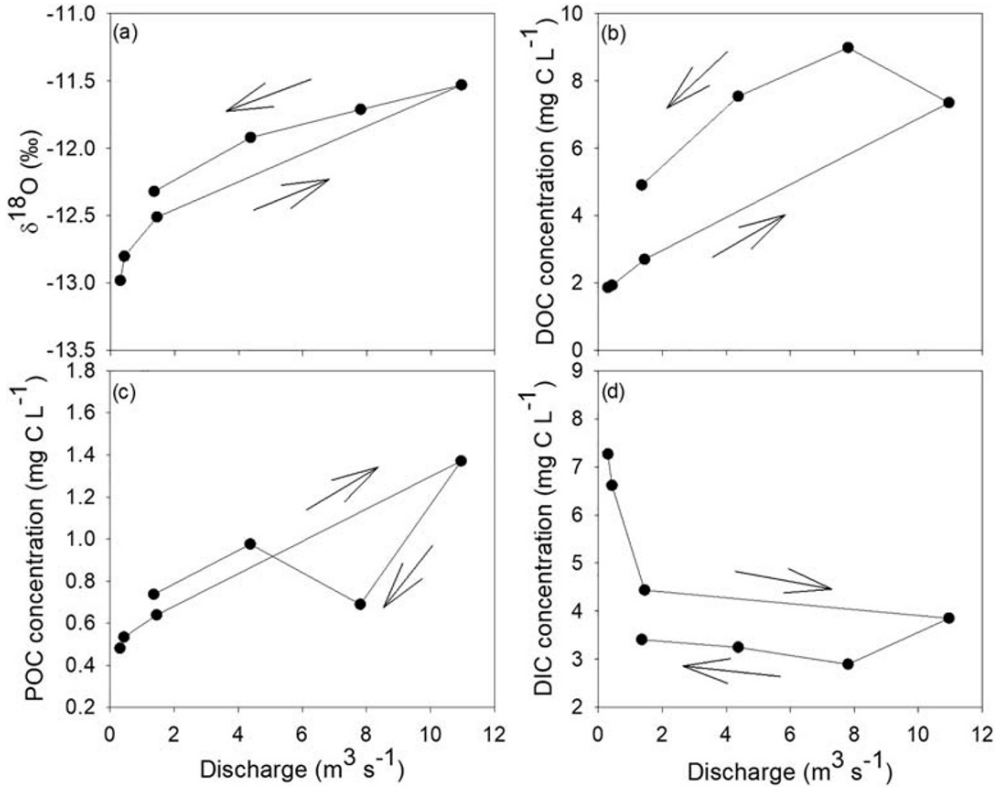


**Figure 3.** Concentration versus discharge plots in the Fish Creek mainstem for (a) $\delta^{18}O$, (b) DOC, (c) POC, and (d) DIC over the course of the storm.

upland forest subcatchment stream, DOC in Fish Creek (CV = 0.59) had a greater CV than POC (CV = 0.40). For all sites together, percent new water was not related to POC concentration ($r^2$ = 0.02, $p$ = 0.476, Figure 4b) but was positively related to DOC:POC ($r^2$ = 0.19, $p$ 0.042, Figure 4c) over the storm.

Concentrations of DIC in the three tributaries varied widely over the storm hydrograph and across sites averaging 7.5 mg C $L^{-1}$ in the poor fen (CV = 1.16), 2.3 mg C $L^{-1}$ in the forested wetland (CV = 0.49), and 15.1 mg C $L^{-1}$ (CV = 0.18) in the upland forest (Figures 2d–2f). Dissolved $CO_2$ dominated the DIC pool in the poor fen and forested wetland but contributed proportionally less in the upland forest and Fish Creek mainstem (Supporting Information Table S1). All three tributaries showed a decrease in DIC concentrations on the ascending limb of the storm hydrograph indicating that DIC concentrations were diluted with increasing discharge (Figures 2d–2f). The largest change in stream water DIC was observed in the poor fen, where concentrations decreased from a prestorm high of 20 mg C $L^{-1}$ to less than 2.0 mg C $L^{-1}$ during peak flow. The observed patterns in C concentrations during the storm resulted in a general increase in DOC:DIC coincident with the enrichment in $\delta^{18}O$ and increased stage height in all tributary streams (data not shown). In Fish Creek, concentrations of DIC showed a strong clockwise hysteresis (HI = 0.32) with concentrations less than 4 mg C $L^{-1}$ on the falling limb of the storm hydrograph (Figure 3d). The contribution of new water was positively related to DIC concentrations ($r^2$ = 0.52, $p < 0.001$, Figure 4d) and ratios of DOC to DIC ($r^2$ = 0.55, $p < 0.001$, Figure 4e) for all sites together.

### 3.3. Hydrologically Driven Shifts in DOM Molecular Composition

Stream water DOM draining the upland forest had the most assigned molecular formulae (7,751–8,720) of the streams, although the number of molecular formulae decreased over the storm and became more similar to the wetland streams (Figure 5a). In contrast, the number of assigned formulae in the two wetland streams varied minimally throughout the storm and ranged from 6,436 to 7,385. The percent relative abundance of sugar-like formulae generally tracked stage height in all tributaries, increasing slightly to peak levels of 0.8% and 1.0% in the poor fen and forested wetland, respectively, before decreasing as flow subsided (Figure 5b;

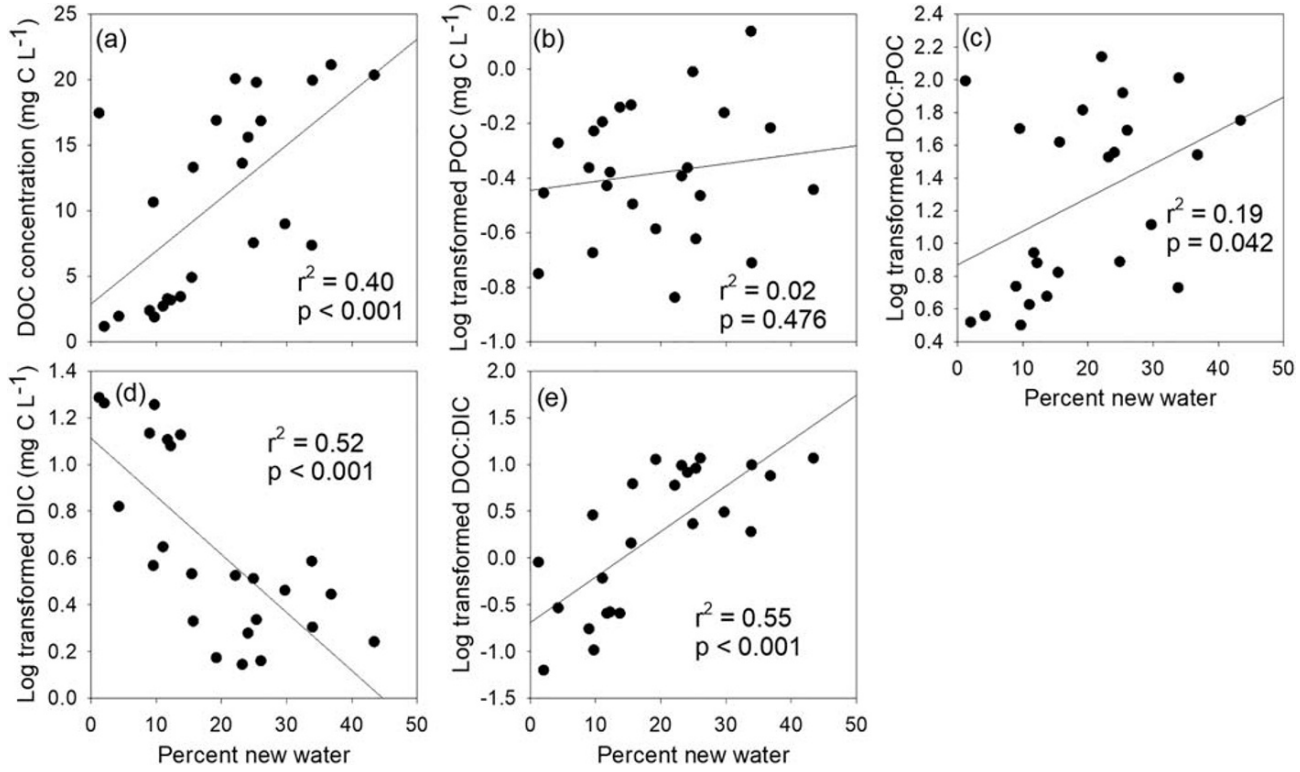


**Figure 4.** Relationship between percent new water and (a) DOC concentration, (b) log transformed POC concentration, (c) log transformed DOC:DIC, (d) log transformed DIC concentration, and (e) log transformed DOC:DIC for all sites together.

Supporting Information Table S2). Similarly, percent relative abundance of aliphatic formulae modestly increased with flow in the upland forest (from 1.0% to 1.9%) and poor fen (1.1% to 1.5%), although aliphatic formulae varied minimally (0.6% to 0.7%) over the storm in the forested wetland (Figure 5c; Supporting Information Table S2).

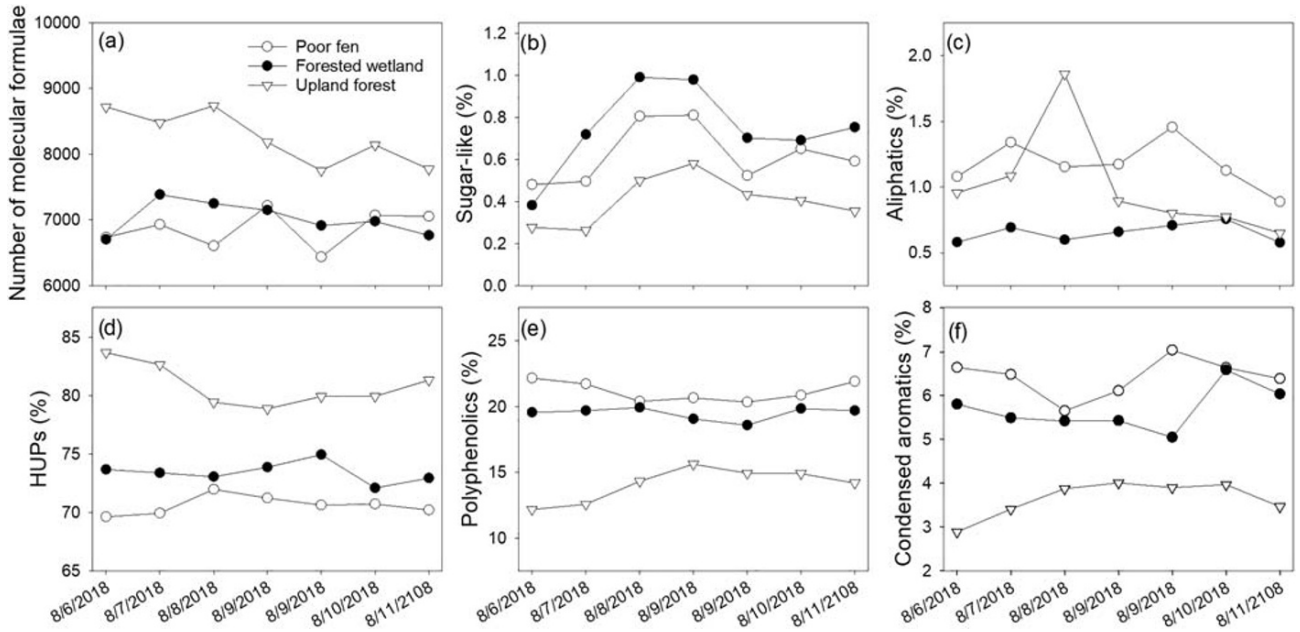


**Figure 5.** Time series of (a) number of molecular formulae, (b) percent relative abundance of sugar-like, (c) percent relative abundance of aliphatics, (d) percent relative abundance of highly unsaturated and phenolics (HUPs), (e) percent relative abundance of polyphenolics, and (f) percent relative abundance of condensed aromatics for the poor fen, forested wetland, and upland forest over the storm (stream water was collected twice on 9 August).

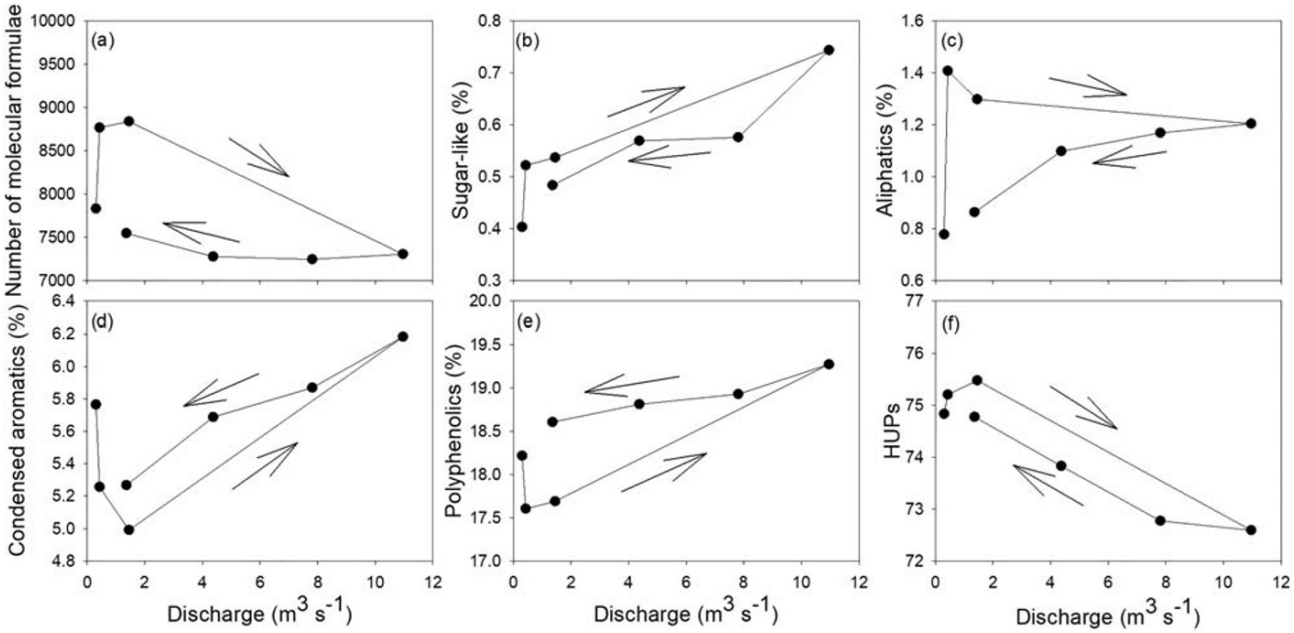


**Figure 6.** Concentration versus discharge plots in the Fish Creek mainstem for (a) number of molecular formulae, (b) percent relative abundance of sugar-like, (c) percent relative abundance of aliphatics, (d) percent relative abundance of polyphenolics, (e) percent relative abundance of condensed aromatics, and (f) percent relative abundance of highly unsaturated and phenolics (HUPs) over the storm.

HUPs contributed the most to DOM in the three tributaries accounting for 70% to 84% of molecular formulae (Figure 5d; Supporting Information Table S2). The remaining molecular formulae were dominated by polyphenolics (12% to 22%) and condensed aromatics (3% to 7%). In the upland forest, percent polyphenolics increased with storm discharge and became more similar to the wetland streams, which varied minimally during the storm (Figure 5e; Supporting Information Table S2). Similarly, percent condensed aromatics increased with peak discharge in the upland forest but decreased in the wetland streams before returning to near prestorm levels on the falling limb of the storm hydrograph (Figure 5f; Supporting Information Table S2). The upland forest showed the greatest variation in DOM molecular composition across all sites, with the percent relative abundance of sugar-like (CV of 0.28) and aliphatic formulae (CV of 0.40) varying the most among all DOM compound classes over the storm hydrograph. However, the CV for all compound classes was generally less than 0.20 across all sites showing modest variation with changes in streamflow.

The weighted average of $AI_{mod}$ (indicating the contribution of aromatic functional groups in DOM; Koch & Dittmar, 2006, 2016) was highest in the wetland streams and varied less with flow relative to the upland forest, where $AI_{mod}$ increased from 0.359 prestorm to 0.379 during peak stormflow (Supporting Information Table S3). The upland forest stream and Fish Creek had the highest relative abundance of heteroatom-containing compounds (CHON mean of 13.1% and 10.3%, respectively, and CHOS/CHONS mean of 8.8% and 4.5%, respectively). The heteroatom contribution to DOM composition in the upland forest and Fish Creek decreased (percent decrease ranged from 60% to 340%) from prestorm conditions through the high flow period, while a severalfold increase in DOM heteroatom content was observed in the poor fen and forested wetland during the storm (Supporting Information Table S3).

In the Fish Creek mainstem, number of molecular formulae showed a strong clockwise hysteresis over the storm hydrograph (HI = 0.13; Figure 6a). The percent relative abundance of sugar-like (HI = 0.09), aliphatics (HI = 0.06), and HUPs (HI = 0.02) similarly showed a clockwise hysteresis in Fish Creek (Figures 6b–6d). In contrast, percent relative abundance polyphenolics (HI = −0.03) and condensed aromatics (HI = −0.05) showed a counterclockwise hysteresis in Fish Creek (Figures 6e and 6f). For all sites together, new water was significantly related to number of molecular formula ($r^2 = 0.42$, $p < 0.001$; Figure 7a), and the percent relative abundance of sugar-like ($r^2 = 0.33$, $p = 0.004$; Figure 7b), HUPs ($r^2 = 0.33$, $p = 0.003$;

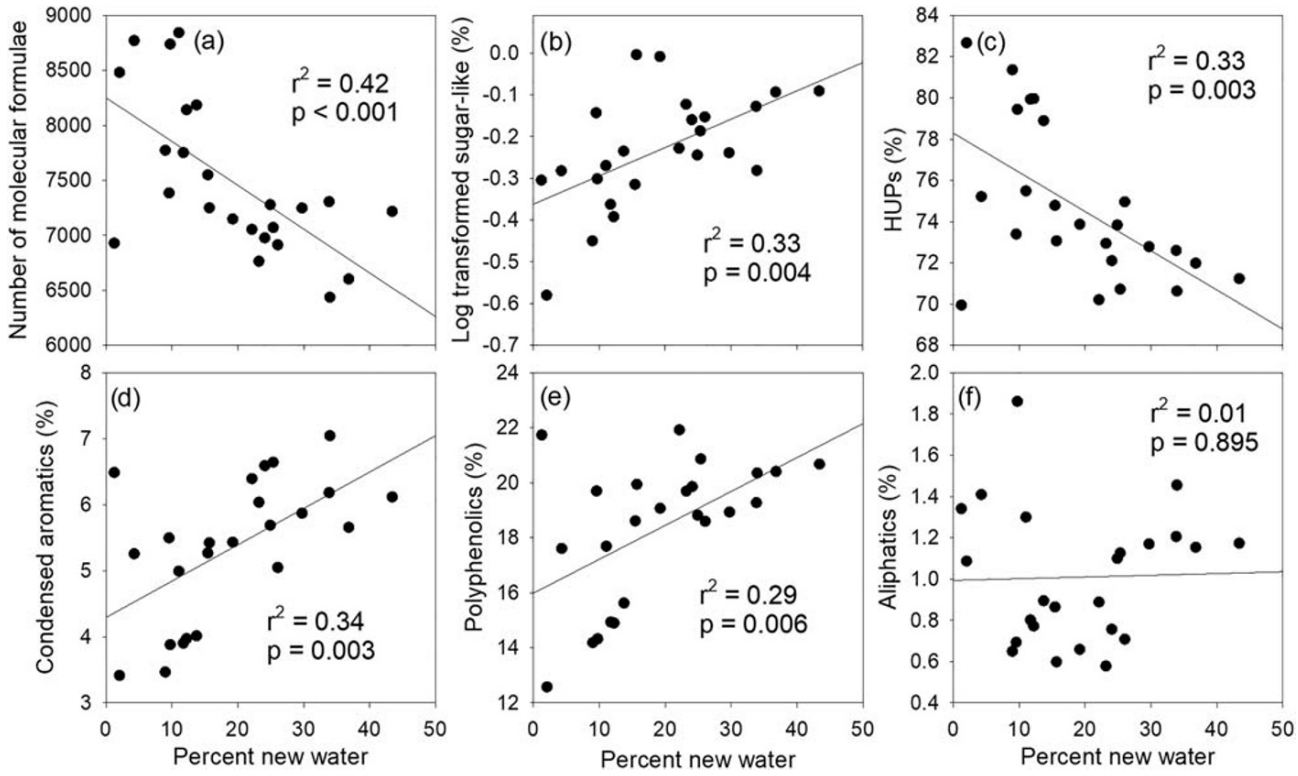


**Figure 7.** Relationship between percent new water and (a) the number of molecular formula, (b) percent relative abundance of sugar-like, (c) percent relative abundance of highly unsaturated and phenolics (HUPs), (d) percent relative abundance of condensed aromatics, (e) percent relative abundance of polyphenolics, and (f) percent relative abundance of aliphatics for all sites together.

Figure 7c), and condensed aromatics ($r^2 = 0.34$, $p = 0.003$; Figure 7d), but not to the relative abundance of polyphenolics ($r^2 = 0.29$, $p = 0.006$; Figure 7e) and aliphatic formulae ($r^2 = 0.01$, $p = 0.895$; Figure 7f).

Prestorm, peak discharge, and poststorm samples (8/6/18, 8/9/18 a.m., and 8/11/18) were examined to assess unique molecular formulae present in only one of the three hydrographic sampling events and in at least two samples from that event to ensure that analysis focused on nonlocalized storm processes (e.g., Spencer et al., 2019; Table 1). Number of molecular formulae identified as unique diminished from prestorm (99) to peak (78) to poststorm (15). The percent relative abundance of aliphatic and sugar-like formulae increased from prestorm to peak storm flow (from 1.01% to 6.41% and 0% to 15.38%, respectively), while neither appeared in the poststorm unique signature. Condensed aromatics, polyphenolics, and HUPs all decreased in relative abundance in the unique formulae between prestorm and peak storm flow, but condensed aromatics and polyphenolics increased as flow receded (Table 1).

**Table 1**
*FT-ICR MS Compound Class Distribution (Number and Percent Relative Abundance) for the Hydrographically Unique Formulae (Present in at Least Two Samples From Each Sampling Event) for the Prestorm, Peak Flow, and Poststorm Sample Dates*

| Compositional region | Prestorm (8/6/2018) | Prestorm (8/9/2018 a.m.) | Poststorm (8/11/2018) |
|---|---|---|---|
| Number of formulae | 99 | 78 | 15 |
| Condensed aromatics # (%) | 9 (9.09) | 1 (1.28) | 1 (6.67) |
| Polyphenolics # (%) | 17 (17.17) | 12 (15.38) | 7 (46.67) |
| HUPs # (%) | 72 (72.73) | 48 (61.54) | 7 (46.67) |
| Aliphatics # (%) | 1 (1.01) | 5 (6.41) | — |
| Sugar-like # (%) | — | 12 (15.38) | — |

*Note.* No formulae from a class present in compositional region indicated by (—).

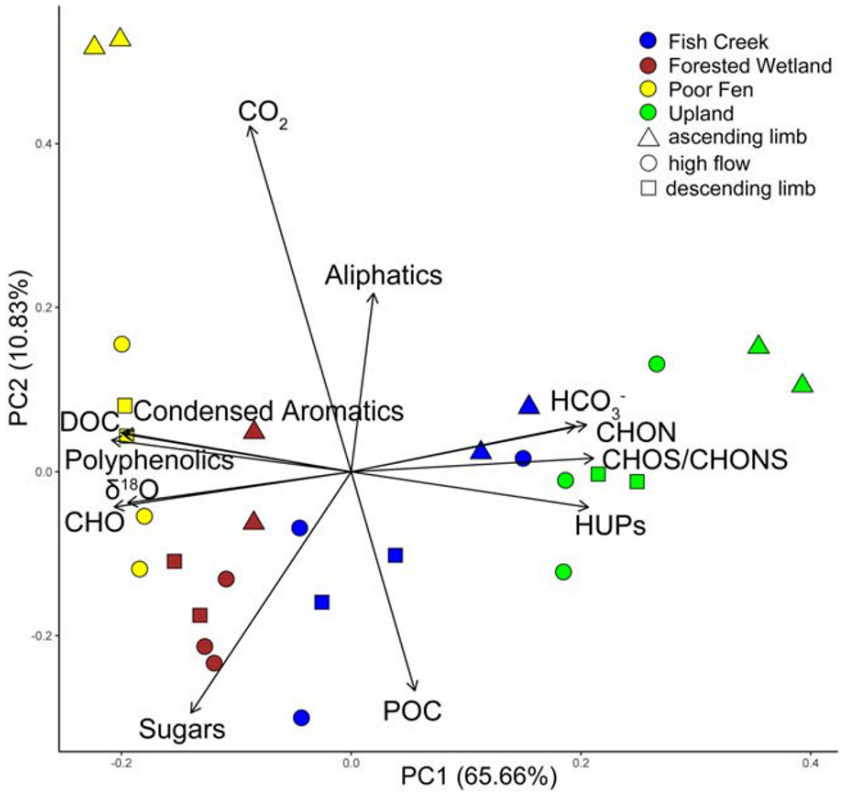


**Figure 8.** The first two factor axes of a PCA of C concentration and speciation and DOM composition for prestorm/ascending limb of the storm hydrograph ($n = 2$ sample points; triangles), high flow period ($n = 3$; circles), and descending storm hydrograph ($n = 2$; squares) for all sites. HUPs stands for highly unsaturated and phenolic molecular formulae.

A PCA of C concentration and DOM composition showed differences in water entering the stream from different landscape types and at different time points during the storm (Figure 8). The first PCA axis explained 66% of the variance in C and DOM biogeochemistry over the course of the storm, while Axis 2 explained 11% of the variance over the storm (Figure 8). Axis 1 separated the two wetland sites from the upland forest and Fish Creek, reflecting greater DOC concentrations, percent polyphenolics, and condensed aromatics and the enrichment of $\delta^{18}O$ in stream water. Furthermore, the upland forest stream had the greatest percent relative abundance of CHON, CHOS, and CHONS containing molecular formulae, HUPs formulae, and $HCO_3^-$, while Fish Creek fell between the wetland sites and upland forest along Axis 1.

Early in the storm, high $CO_2$ concentrations in the poor fen created separation from the forested wetland along Axis 2. However, following peak flow, the two wetland sites became more similar to each other in terms of DOC concentration, $\delta^{18}O$ values, and percent sugar-like, condensed aromatics, and polyphenolics (Figure 8). During the ascending limb, the upland forest and Fish Creek separated from the other sites on Axis 1 due to high $HCO_3^-$ concentrations and heteroatom-rich, HUPs-rich molecular formulae, while later in the storm Fish Creek grouped more closely with the wetland streams. Fish Creek showed the largest spread along Axis 1 consistent with diverse organic matter inputs from the three landscape types during the storm.

## 4. Discussion

### 4.1. Hydrologic Controls on C Speciation and Export

Our findings support the extensive body of work showing that rainfall events strongly impact the concentration and form of C exported from forested and wetland catchments (Hornberger et al., 1994; Leach et al., 2016; Peter et al., 2014; Salimon et al., 2013). In this study, percent new water was significantly

related to concentrations of DOC and DIC for all sites together, providing a clear link between contributing sources of stream water (i.e., recent rain water) and C concentrations and form. This recent event water likely entered the tributary streams through shallow subsurface flow paths and/or via saturation-excess overland flow (mainly in wetland sites) given that previous research from the PCTR (D'Amore et al., 2015; Emili & Price, 2006) and other forested regions (Boyer et al., 1997; Hinton et al., 1997; Peralta-Tapia et al., 2015; van Meerveld et al., 2015) shows that streamflow is generated rapidly when soil water table levels are elevated into hydrologically conductive soil surface horizons. These explicit linkages between water and terrestrial C sources provide one of the few examples in northern forested watersheds where tight catchment-scale coupling between the water and C cycles has been observed (Tomco et al., 2019).

It is well recognized that soil hydrologic flow paths control C delivery to surface waters (Duvert et al., 2018; Hinton et al., 1997; Senar et al., 2018; Worrall et al., 2002). During storms when the water table is elevated into the soil surface horizons, the dominant flow paths for water moving into the stream switch from predominantly deeper flow paths to mainly upper soil horizons resulting in the flushing of abundant DOC (Raymond et al., 2016; Senar et al., 2018) and POC (Goni et al., 2013) to surface waters. In the PCTR, this results in high DOC yields, particularly from wetlands during the late summer and fall wet season (D'Amore et al., 2015; Fellman et al., 2009; Oliver et al., 2017) when frontal storms moving off the Gulf of Alaska (GOA) deliver large amounts of rainfall to southeast Alaska. In our study subcatchments, hydrologic connectivity between terrestrial C source pools and stream water appears to limit the delivery of DOC to surface water rather than C supply because concentrations increased with discharge. This transport limitation is consistent with many forested watersheds in the United States, which show a similar response in DOC concentrations during rainfall events (Zarnetske et al., 2018). Furthermore, the DOC concentrations observed here and in a previous study of high flow events in the region (Fellman et al., 2009) were not diluted with increasing flow. These results are counter to previous studies of northern wetlands showing dilution of stream water DOC during high flow events such as spring snowmelt (Ågren et al., 2007; Eimers et al., 2007; Fraser et al., 2001; Laudon et al., 2011) and midsummer stormflows (Worrall et al., 2008). It is possible that some sort of cumulative threshold for rainfall (which this storm did not reach), repeated rainfall events that dilute soil DOC pools, or elevated prestorm DOC concentrations are necessary for DOC dilution to occur in wetland streams in the PCTR.

Stream water POC concentrations increased with flow in all sites (especially in the poor fen), although POC still contributed very little to the bulk pool of stream water C during the storm. These results support previous studies of northern peatlands that show that POC export is generally quite low except when bare peat surfaces are exposed (Dawson et al., 2004; Evans et al., 2016). The poor fen had a considerably larger CV for POC than DOC and likely indicates different mechanisms involved in POC generation and delivery to surface water compared to DOC. In temperate forested streams, stormflow sampling showed that POC is transported to surface water mainly through surface runoff while DOC is mobilized through the leaching of soil surface horizons and saturation overland flow (Dhillon & Inamdar, 2014). Thus, the small spike in POC in the poor fen could be from the flushing of plant material from the soil surface to the stream via surface runoff during the storm.

Stream water DIC concentrations exhibited maxima during prestorm baseflow conditions, supporting previous research showing that elevated DIC concentrations typically occur during periods of low streamflow when soil water tables are depressed and hydrologic flow paths are predominantly located in deeper soil horizons (Dinsmore & Billett, 2008; Leach et al., 2016; Peter et al., 2014). Although the continuous production of DIC from soil respiration (both autotrophic and heterotrophic) can lead to a buildup of $CO_2$ in soil waters that is slowly delivered to surface water (Campeau et al., 2019; Johnson et al., 2008; Winterdahl et al., 2016), DIC concentrations were diluted in the tributary streams (especially in the poor fen) during peak flows indicating that DIC production (mostly through $CO_2$ generation) in the soil profile did not keep pace with increasing discharge. Storm and high discharge events have similarly been shown to dilute stream DIC concentrations in forested (Peter et al., 2014), peatland (Dinsmore & Billett, 2008), and large Arctic catchments (Drake et al., 2018), although stream $pCO_2$ concentrations have also been shown to increase during the rainy season in tropical catchments (Salimon et al., 2013). It was not until later in the storm when deeper flow paths likely became an increasingly important contributor to streamflow that a subtle increase in DIC concentration was observed. In some forested catchments, it can take up to 6 days for DIC concentration to recover to near prestorm levels (Peter et al., 2014). Overall, our findings suggest that during the storm, DIC

delivery to stream water was source rather than transport limited, with DIC concentrations controlled by the balance between the production and transport of DIC to surface water across the storm hydrograph.

Lateral C loss is commonly excluded from terrestrial ecosystem-scale C balance studies because it is generally thought to be a minor component of net ecosystem production (Abril & Borges, 2019; McGuire et al., 2000; Trumbore, 2006). However, considerable overestimation of terrestrial C uptake could occur by not accounting for the dissolution of soil respiration and subsequent export as DIC to surface waters (Abril & Borges, 2019; Butman et al., 2016). Our finding that DIC concentrations were especially high in the poor fen early in the storm suggests that lateral DIC could be an important contributor to the C balance of wetland and forested ecosystems in the region. Future research quantifying relative DIC losses via lateral versus vertical (soil respiration) pathways would elucidate the proportion of soil respiration that was transported laterally as dissolved C in PCTR watersheds.

### 4.2. Landscape Controls on C Export

Although the limited collection of daily samples prevented robust linkages between C export and contributing hydrologic flow paths, our findings provide a framework for evaluating linked hydro-biogeochemical processes that control C production and transport across the terrestrial-aquatic interface. For instance, percent new water was significantly related to DOM molecular compound classes in all sites, supporting the notion that recent event water entering the stream through shallow subsurface flow paths entrains abundant DOM enriched in plant-derived molecular compound classes (O'Donnell et al., 2016; C. S. Shanley et al., 2015; Spencer et al., 2015). Much of this DOM enriched in polyphenolics and condensed aromatics likely originated from tight hydrologic connectivity between the Fish Creek mainstem and cryptic wetlands interspersed within the catchment (Creed et al., 2003) and/or the poor fen and forested wetland landcover located within the catchment (Figure 8). In contrast, isotopic hydrograph separation showed that water entering the stream early in the storm was likely from pre-event water draining upland forest landcover in the catchment that was delivering comparatively older water with high molecular diversity (Figure 7a).

The molecular properties of DOM in the stream draining the upland forest converged on those of the wetland sites during the storm (except for percent aliphatic and sugar-like formulae). These findings are consistent with other temperate and tropical forested and agricultural watersheds showing elevated export of aromatic molecular formulae (e.g., condensed aromatics and polyphenolics, and as indicated by $AI_{mod}$) during high flow events (Eckard et al., 2017; Spencer et al., 2019; Wagner et al., 2019). The upland forest had the greatest CV for DOC and POC suggesting that organic forms of C vary more in uplands during storms than in the wetland streams, which in turn showed the greatest variation in DIC over the storm. Thus, higher organic C export per volume of water was observed in the upland forest compared to the poor fen and forested wetland. Similarly, the DOM exported from the upland forest had the greatest molecular diversity, heteroatom content (N and S), and CV for DOM molecular compound classes of the landcover types suggesting that the wetland sites were less compositionally diverse with regard to soil DOM export over the storm.

Percent relative abundance of aliphatic and sugar-like formulae generally increased with flow in all sites, implying tight connectivity between recently leached soil surface C pools and stream water (Fellman et al., 2009). This recently leached DOM that was rapidly flushed to surface water by recent event water represents a potential energetic subsidy to downstream and coastal marine ecosystems because these moieties are highly biolabile to stream microbial communities (Berggren et al., 2010; Spencer et al., 2015; Textor et al., 2018). Further, the increase in unique energy-rich formulae (aliphatics and sugar-like) during high discharge (Table 1) shows how storm events can shunt biolabile compounds downstream (Raymond et al., 2016) that otherwise would be consumed by microbial communities in soils or headwater reaches. Thus, the impact of terrestrial DOM subsidies on downstream and nearshore metabolic processes may be at its peak during or shortly after stormflows.

Catchment landscape heterogeneity is one of the main mechanisms controlling stream C biogeochemistry because landcover impacts the molecular composition (Mosher et al., 2015; Seifert et al., 2016; Spencer et al., 2019) as well as the magnitude and partitioning of C exported across the terrestrial-aquatic interface (Ågren et al., 2014; Goni et al., 2013; Perdrial et al., 2014). In our study, stream water DOC:DIC generally decreased along the hydric soil gradient (poor fen-forested wetland-upland forest) during peak flows resulting in DOC comprising a decreasing fraction of lateral C concentrations from the more highly drained

upland forest soils during the storm. Furthermore, the abundance of heteroatom-containing DOM in Fish Creek likely reflects multiple catchment sources of DOM draining into the mainstem during the storm. The fact that the DOM molecular properties in Fish Creek reflected all three landcover types to varying extents and at various points of the storm hydrograph supports the notion that the DOM composition of individual landscape types (wetlands, forest) becomes less distinct along the fluvial network (Laudon et al., 2011; Spencer et al., 2015; Tiwari et al., 2014). Although processing and removal (either through sorption or emission to the atmosphere) of C and DOM occur along fluvial networks (Creed et al., 2015; Hotchkiss et al., 2015; Spencer et al., 2015) and limit interpretation, we suggest that stream water DOM molecular properties at catchment outlets are controlled in part by the interactive effects of water routing through soils and the diversity of DOM source pools in distinct landcover types, such as wetlands (Coble et al., 2019; Wilson & Xenopoulos, 2009).

### 4.3. Climate Controls on C Export

Lateral C export during high flow events has also been shown to vary with season, with higher C export per volume of water expected to occur during summer months, particularly after extended dry periods (Inamdar et al., 2011; Vaughan et al., 2019; Worrall et al., 2008). The fact that we sampled only a single event storm limits our interpretation to the summer season and from making detailed comparisons on concentration-discharge relationships with other studies. Further work is needed to intensively sample storms under different temperature (summer vs. winter) and hydrologic regimes (saturated vs. unsaturated antecedent soil moisture conditions) to determine how seasonal changes in climate impact the magnitude and partitioning of lateral C export as well as how DOM molecular compound classes routinely respond to a range of storms over the year. This information could provide a more nuanced understanding of how climate-driven hydrologic regime shifts will impact episodic and annual lateral C export in the region.

Climate in the PCTR is projected to become warmer and wetter in coming decades (C. S. Shanley et al., 2015; Wang et al., 2012), with a variety of impacts on hydrological fluxes. These projections imply that coastal ecosystems in the region will be subject to larger storm events with more precipitation falling as rain rather than snow (Barnett et al., 2005), leading to greater winter discharge, reduced spring snowmelt, and more pronounced summer drying (C. S. Shanley et al., 2015). Our findings suggest that future changes in rainfall intensity will increase the frequency of high flow events that export a large fraction of young streamflow (driven by rain during the event). This change in hydrology will likely shift the ratio between DOC and DIC such that DOC comprises a larger proportion of annual lateral C loss (relative to DIC) from forested catchments in the region. Shifts in precipitation falling as rain rather than snow could also result in a greater frequency of rain-on-snow events (Musselman et al., 2018) and an increased fraction of annual lateral C export occurring during winter stormflows, which are poorly understood in high-latitude forested catchments. All of these expected changes in hydrologic forcing likely have notable and largely unquantified implications for stream C export from PCTR ecosystems.

## 5. Conclusions

Our findings highlight the importance of quantifying all forms of lateral C export in catchment-scale C studies. The results from the isotopic hydrograph separation demonstrate that DOM compound classes may behave independently of each other, suggesting a strong source control on stream water DOM composition. This study provides a framework for quantifying lateral C export from forested catchments in the context of a changing hydrologic regime and, in particular, contributes to our understanding of whether C export and speciation is limited by C production in the terrestrial ecosystem or by a lack of hydrologic connectivity (i.e., flow paths) between C source pools and surface waters. Furthermore, our findings suggest that integrating measurements of all C forms with hydrologic flow path information, which laterally connect and route terrestrial C to fluvial systems, could improve terrestrial ecosystem C budgets that typically focus more on atmospheric emission of $CO_2$ rather than high-resolution quantification of lateral C fluxes.

## Data Availability Statement

Data archiving through DataONE "Environmental Data Initiative" are underway. All data included in this manuscript are available online (at http://www.doi.org/10.5063/F19885C1).

**Acknowledgments**

We thank Emily Whitney of the University of Alaska Southeast for field and laboratory assistance. This study received support from the University of Alaska Faculty Initiative Fund. A portion of this work was performed at the National High Magnetic Field Laboratory ICR User Facility, which is supported by the National Science Foundation Division of Chemistry through DMR-1644779 and DMR-1157490 and the State of Florida. J. F. and E. H. also received support from National Science Foundation (NSF) under Award OIA-1753748.

## References

Abril, G., & Borges, A. V. (2019). Ideas and perspectives: Carbon leaks from flooded land: Do we need to replumb the inland water active pipe? *Biogeosciences*, *16*(3), 769–784. https://doi.org/10.5194/bg-16-769-2019

Ågren, A., Buffam, I., Jansson, M., & Laudon, H. (2007). Importance of seasonality and small streams for the landscape regulation of dissolved organic carbon export. *Journal of Geophysical Research*, *112*(G3), n/a. https://doi.org/10.1029/2006JG000381

Ågren, A. M., Buffam, I., Cooper, D. M., Tiwari, T., Evans, C. D., & Laudon, H. (2014). Can the heterogeneity in stream dissolved organic carbon be explained by contributing landscape elements? *Biogeosciences*, *11*(4), 1199–1213. https://doi.org/10.5194/bg-11-1199-2014

Argerich, A., Haggerty, R., Johnson, S. L., Wondzell, S. M., Dosch, N., Corson-Rikert, H., et al. (2016). Comprehensive multiyear carbon budget of a temperate headwater stream: Carbon budget of a headwater stream. *Journal of Geophysical Research: Biogeosciences*, *121*(5), 1306–1315. https://doi.org/10.1002/2015JG003050

Barnett, T. P., Adam, J. C., & Lettenmaier, D. P. (2005). Potential impacts of a warming climate on water availability in snow-dominated regions. *Nature*, *438*(7066), 303–309. https://doi.org/10.1038/nature04141

Battin, T. J., Luyssaert, S., Kaplan, L. A., Aufdenkampe, A. K., Richter, A., & Tranvik, L. J. (2009). The boundless carbon cycle. *Nature Geoscience*, *2*(9), 598–600. https://doi.org/10.1038/ngeo618

Benettin, P., Bailey, S. W., Campbell, J. L., Green, M. B., Rinaldo, A., Likens, G. E., et al. (2015). Linking water age and solute dynamics in streamflow at the Hubbard Brook Experimental Forest, NH, USA. *Water Resources Research*, *51*(11), 9256–9272. https://doi.org/10.1002/2015WR017552

Berggren, M., Laudon, H., Haei, M., Ström, L., & Jansson, M. (2010). Efficient aquatic bacterial metabolism of dissolved low-molecular-weight compounds from terrestrial sources. *The ISME Journal*, *4*(3), 408–416. https://doi.org/10.1038/ismej.2009.120

Boyer, E. W., Hornberger, G. M., Bencala, K. E., & McKnight, D. M. (1997). Response characteristics of DOC flushing in an alpine catchment. *Hydrological Processes*, *11*(12), 1635–1647. https://doi.org/10.1002/(SICI)1099-1085(19971015)11:121635::AID-HYP494>3.0.CO;2-H

Butman, D., Stackpoole, S., Stets, E., McDonald, C. P., Clow, D. W., & Striegl, R. G. (2016). Aquatic carbon cycling in the conterminous United States and implications for terrestrial carbon accounting. *Proceedings of the National Academy of Sciences*, *113*(1), 58–63. https://doi.org/10.1073/pnas.1512651112

Butman, D., Striegl, R., Stackpoole, S., del Giorgio, P., Prairie, Y., Pilcher, D., et al. (2018). Chapter 14: Inland waters. Second State of the Carbon Cycle Report. U.S. Global Change Research Program. https://doi.org/10.7930/SOCCR2.2018.Ch14

Campeau, A., Bishop, K., Amvrosiadi, N., Billett, M. F., Garnett, M. H., Laudon, H., et al. (2019). Current forest carbon fixation fuels stream $CO_2$ emissions. *Nature Communications*, *10*(1), 1876. https://doi.org/10.1038/s41467-019-09922-3

Coble, A. A., Koenig, L. E., Potter, J. D., Parham, L. M., & McDowell, W. H. (2019). Homogenization of dissolved organic matter within a river network occurs in the smallest headwaters. *Biogeochemistry*, *143*(1), 85–104. https://doi.org/10.1007/s10533-019-00551-y

Cole, J. J., Prairie, Y. T., Caraco, N. F., McDowell, W. H., Tranvik, L. J., Striegl, R. G., et al. (2007). Plumbing the global carbon cycle: Integrating inland waters into the terrestrial carbon budget. *Ecosystems*, *10*(1), 172–185. https://doi.org/10.1007/s10021-006-9013-8

Connelly, T., McClelland, J., Crump, B., Kellogg, C., & Dunton, K. (2015). Seasonal changes in quantity and composition of suspended particulate organic matter in lagoons of the Alaskan Beaufort Sea. *Marine Ecology Progress Series*, *527*, 31–45. https://doi.org/10.3354/meps11207

Creed, I. F., McKnight, D. M., Pellerin, B. A., Green, M. B., Bergamaschi, B. A., Aiken, G. R., et al. (2015). The river as a chemostat: Fresh perspectives on dissolved organic matter flowing down the river continuum. *Canadian Journal of Fisheries and Aquatic Sciences*, *72*(8), 1272–1285. https://doi.org/10.1139/cjfas-2014-0400

Creed, I. F., Sanford, S. E., Beall, F. D., Molot, L. A., & Dillon, P. J. (2003). Cryptic wetlands: Integrating hidden wetlands in regression models of the export of dissolved organic carbon from forested landscapes. *Hydrological Processes*, *17*(18), 3629–3648. https://doi.org/10.1002/hyp.1357

Csank, A. Z., Czimczik, C. I., Xu, X., & Welker, J. M. (2019). Seasonal patterns of riverine carbon sources and export in NW Greenland. *Journal of Geophysical Research: Biogeosciences*, *124*(4), 840–856. https://doi.org/10.1029/2018JG004895

D'Amore, D. V., Edwards, R. T., Herendeen, P. A., Hood, E., & Fellman, J. B. (2015). Dissolved organic carbon fluxes from hydropedologic units in Alaskan coastal temperate rainforest watersheds. *Soil Science Society of America Journal*, *79*(2), 378–388. https://doi.org/10.2136/sssaj2014.09.0380

D'Amore, D. V., Fellman, J. B., Edwards, R. T., & Hood, E. (2010). Controls on dissolved organic matter concentrations in soils and streams from a forested wetland and sloping bog in southeast Alaska. *Ecohydrology*, *3*(3), 249–261. https://doi.org/10.1002/eco.101

Dawson, J. J. C., Billett, M. F., Hope, D., Palmer, S. M., & Deacon, C. M. (2004). Sources and sinks of aquatic carbon in a peatland stream continuum. *Biogeochemistry*, *70*(1), 71–92. https://doi.org/10.1023/B:BIOG.0000049337.66150.f1

Dhillon, G. S., & Inamdar, S. (2014). Storm event patterns of particulate organic carbon (POC) for large storms and differences with dissolved organic carbon (DOC). *Biogeochemistry*, *118*(1–3), 61–81. https://doi.org/10.1007/s10533-013-9905-6

Dinsmore, K. J., & Billett, M. F. (2008). Continuous measurement and modeling of $CO_2$ losses from a peatland stream during stormflow events. *Water Resources Research*, *44*. https://doi.org/10.1029/2008WR007284

Dittmar, T., Koch, B., Hertkorn, N., & Kattner, G. (2008). A simple and efficient method for the solid-phase extraction of dissolved organic matter (SPE-DOM) from seawater: SPE-DOM from seawater. *Limnology and Oceanography: Methods*, *6*(6), 230–235. https://doi.org/10.4319/lom.2008.6.230

Drake, T. W., Raymond, P. A., & Spencer, R. G. M. (2017). Terrestrial carbon inputs to inland waters: A current synthesis of estimates and uncertainty: Terrestrial carbon inputs to inland waters. *Limnology and Oceanography Letters.*, *3*(3), 132–142. https://doi.org/10.1002/lol2.10055

Drake, T. W., Tank, S. E., Zhulidov, A. V., Holmes, R. M., Gurtovaya, T., & Spencer, R. G. M. (2018). Increasing alkalinity export from large Russian Arctic rivers. *Environmental Science & Technology*, *52*(15), 8302–8308. https://doi.org/10.1021/acs.est.8b01051

Duvert, C., Butman, D. E., Marx, A., Ribolzi, O., & Hutley, L. B. (2018). $CO_2$ evasion along streams driven by groundwater inputs and geomorphic controls. *Nature Geoscience*, *11*(11), 813–818. https://doi.org/10.1038/s41561-018-0245-y

Eckard, R. S., Pellerin, B. A., Bergamaschi, B. A., Bachand, P. A. M., Bachand, S. M., Spencer, R. G. M., & Hernes, P. J. (2017). Dissolved organic matter compositional change and biolability during two storm runoff events in a small agricultural watershed. *Journal of Geophysical Research: Biogeosciences*, *122*(10), 2634–2650. https://doi.org/10.1002/2017JG003935

Eimers, M. C., Watmough, S. A., Buttle, J. M., & Dillon, P. J. (2007). Examination of the potential relationship between droughts, sulphate and dissolved organic carbon at a wetland-draining stream. *Global Change Biology*, *14*(4), 938–948. https://doi.org/10.1111/j.1365-2486.2007.01530.x

Emili, L. A., & Price, J. S. (2006). Hydrological processes controlling ground and surface water flow from a hypermaritime forest–peatland complex, Diana Lake Provincial Park, British Columbia, Canada. *Hydrological Processes*, *20*(13), 2819–2837. https://doi.org/10.1002/hyp.6077

Evans, C. D., Renou-Wilson, F., & Strack, M. (2016). The role of waterborne carbon in the greenhouse gas balance of drained and re-wetted peatlands. *Aquatic Sciences*, *78*(3), 573–590. https://doi.org/10.1007/s00027-015-0447-y

Fellman, J. B., D'Amore, D. V., Hood, E., & Boone, R. D. (2008). Fluorescence characteristics and biodegradability of dissolved organic matter in forest and wetland soils from coastal temperate watersheds in southeast Alaska. *Biogeochemistry*, *88*(2), 169–184. https://doi.org/10.1007/s10533-008-9203-x

Fellman, J. B., Hood, E., Edwards, R. T., & D'Amore, D. V. (2009). Changes in the concentration, biodegradability, and fluorescent properties of dissolved organic matter during stormflows in coastal temperate watersheds. *Journal of Geophysical Research*, *114*(G1), G01021. https://doi.org/10.1029/2008JG000790

Fraser, C. J. D., Roulet, N. T., & Moore, T. R. (2001). Hydrology and dissolved organic carbon biogeochemistry in an ombrotrophic bog. *Hydrological Processes*, *15*(16), 3151–3166. https://doi.org/10.1002/hyp.322

Genereux, D. (1998). Quantifying uncertainty in tracer-based hydrograph separations. *Water Resources Research*, *34*(4), 915–919. https://doi.org/10.1029/98WR00010

Goni, M. A., Hatten, J. A., Wheatcroft, R. A., & Borgeld, J. C. (2013). Particulate organic matter export by two contrasting small mountainous rivers from the Pacific Northwest, U.S.A. *Journal of Geophysical Research: Biogeosciences*, *118*(1), 112–134. https://doi.org/10.1002/jgrg.20024

Hendrickson, C. L., Quinn, J. P., Kaiser, N. K., Smith, D. F., Blakney, G. T., Chen, T., et al. (2015). 21 tesla Fourier transform ion cyclotron resonance mass spectrometer: A national resource for ultrahigh resolution mass analysis. *Journal of the American Society for Mass Spectrometry*, *26*(9), 1626–1632. https://doi.org/10.1007/s13361-015-1182-2

Hinton, M. J., Schiff, S. L., & English, M. (1997). The significance of storms for the concentration and export of dissolved organic carbon from two Precambrian Shield catchments. *Biogeochemistry*, *36*(1), 67–88. https://doi.org/10.1023/A:1005779711821

Holmes, R. M., McClelland, J. W., Peterson, B. J., Tank, S. E., Bulygina, E., Eglinton, T. I., et al. (2012). Seasonal and annual fluxes of nutrients and organic matter from large rivers to the Arctic Ocean and surrounding seas. *Estuaries and Coasts*, *35*(2), 369–382. https://doi.org/10.1007/s12237-011-9386-6

Hood, E., Gooseff, M. N., & Johnson, S. L. (2006). Changes in the character of stream water dissolved organic carbon during flushing in three small watersheds, Oregon. *Journal of Geophysical Research*, *111*(G1), G01007. https://doi.org/10.1029/2005JG000082

Hornberger, G. M., Bencala, K. E., & McKnight, D. M. (1994). Hydrological controls on dissolved organic carbon during snowmelt in the Snake River near Montezuma, Colorado. *Biogeochemistry*, *25*(3), 147–165. https://doi.org/10.1007/BF00024390

Hotchkiss, E. R., Hall, R. O. Jr., Sponseller, R. A., Butman, D., Klaminder, J., Laudon, H., et al. (2015). Sources of and processes controlling $CO_2$ emissions change with the size of streams and rivers. *Nature Geoscience*, *8*(9), 696–699. https://doi.org/10.1038/ngeo2507

Inamdar, S., Singh, S., Dutta, S., Levia, D., Mitchell, M., Scott, D., et al. (2011). Fluorescence characteristics and sources of dissolved organic matter for stream water during storm events in a forested mid-Atlantic watershed. *Journal of Geophysical Research*, *116*(G3), G03043. https://doi.org/10.1029/2011JG001735

Johnson, M. S., Lehmann, J., Riha, S. J., Krusche, A. V., Richey, J. E., Ometto, J. P. H. B., & Couto, E. G. (2008). $CO_2$ efflux from Amazonian headwater streams represents a significant fate for deep soil respiration. *Geophysical Research Letters*, *35*, L17401. https://doi.org/10.1029/2008GL034619

Kassambara, A., & Mundt, F. (2017). Factoextra: Extract and visualize the results of multivariate data analyses. *R Package Version*, *1*(5), 337–354. Retrieved from https://CRAN.R-project.org/package=factoextra

Kirchner, J. W. (2016). Aggregation in environmental systems—Part 1: Seasonal tracer cycles quantify young water fractions, but not mean transit times, in spatially heterogeneous catchments. *Hydrology and Earth System Sciences*, *20*(1), 279–297. https://doi.org/10.5194/hess-20-279-2016

Klaus, J., & McDonnell, J. J. (2013). Hydrograph separation using stable isotopes: Review and evaluation. *Journal of Hydrology*, *505*, 47–64. https://doi.org/10.1016/j.jhydrol.2013.09.006

Koch, B. P., & Dittmar, T. (2006). From mass to structure: An aromaticity index for high-resolution mass data of natural organic matter. *Rapid Communications in Mass Spectrometry*, *20*(5), 926–932. https://doi.org/10.1002/rcm.2386

Koch, B. P., & Dittmar, T. (2016). From mass to structure: An aromaticity index for high-resolution mass data of natural organic matter. *Rapid Communications in Mass Spectrometry*, *30*(1), 250–250. https://doi.org/10.1002/rcm.7433

Koch, B. P., Dittmar, T., Witt, M., & Kattner, G. (2007). Fundamentals of molecular formula assignment to ultrahigh resolution mass data of natural organic matter. *Analytical Chemistry*, *79*(4), 1758–1763. https://doi.org/10.1021/ac061949s

Laudon, H., Berggren, M., Ågren, A., Buffam, I., Bishop, K., Grabs, T., et al. (2011). Patterns and dynamics of dissolved organic carbon (DOC) in boreal streams: The role of processes, connectivity, and scaling. *Ecosystems*, *14*(6), 880–893. https://doi.org/10.1007/s10021-011-9452-8

Laudon, H., Kohler, S., & Buffam, I. (2004). Seasonal TOC export from seven boreal catchments in northern Sweden. *Aquatic Sciences - Research Across Boundaries*, *66*(2), 223–230. https://doi.org/10.1007/s00027-004-0700-2

Lawler, D. M., Petts, G. E., Foster, I. D. L., & Harper, S. (2006). Turbidity dynamics during spring storm events in an urban headwater river system: The Upper Tame, West Midlands, UK. *Science of the Total Environment*, *360*(1–3), 109–126. https://doi.org/10.1016/j.scitotenv.2005.08.032

Leach, J. A., Larsson, A., Wallin, M. B., Nilsson, M. B., & Laudon, H. (2016). Twelve year interannual and seasonal variability of stream carbon export from a boreal peatland catchment: Peatland stream carbon export. *Journal of Geophysical Research: Biogeosciences*, *121*(7), 1851–1866. https://doi.org/10.1002/2016JG003357

McGuire, A. D., Clein, J. S., Melillo, J. M., Kicklighter, D. W., Meier, R. A., Vorosmarty, C. J., & Serreze, M. C. (2000). Modelling carbon responses of tundra ecosystems to historical and projected climate: Sensitivity of pan-Arctic carbon storage to temporal and spatial variation in climate. *Global Change Biology*, *6*(S1), 141–159. https://doi.org/10.1046/j.1365-2486.2000.06017.x

McNicol, G., Bulmer, C., D'Amore, D., Sanborn, P., Saunders, S., Giesbrecht, I., et al. (2019). Large, climate-sensitive soil carbon stocks mapped with pedology-informed machine learning in the North Pacific coastal temperate rainforest. *Environmental Research Letters*, *14*(1), 014004. https://doi.org/10.1088/1748-9326/aaed52

van Meerveld, H. J., Seibert, J., & Peters, N. E. (2015). Hillslope-riparian-stream connectivity and flow directions at the Panola Mountain Research Watershed. *Hydrological Processes*, *29*(16), 3556–3574. https://doi.org/10.1002/hyp.10508

Moatar, F., Abbott, B. W., Minaudo, C., Curie, F., & Pinay, G. (2017). Elemental properties, hydrology, and biology interact to shape concentration-discharge curves for carbon, nutrients, sediment, and major ions. *Water Resources Research*, *53*(2), 1270–1287. https://doi.org/10.1002/2016WR019635

Mosher, J. J., Kaplan, L. A., Podgorski, D. C., McKenna, A. M., & Marshall, A. G. (2015). Longitudinal shifts in dissolved organic matter chemogeography and chemodiversity within headwater streams: A river continuum reprise. *Biogeochemistry*, *124*(1–3), 371–385. https://doi.org/10.1007/s10533-015-0103-6

Musselman, K. N., Lehner, F., Ikeda, K., Clark, M. P., Prein, A. F., Liu, C., et al. (2018). Projected increases and shifts in rain-on-snow flood risk over western North America. *Nature Climate Change*, *8*(9), 808–812. https://doi.org/10.1038/s41558-018-0236-4

National Wetlands Working Group. (1988). *Wetlands of Canada*, *Ecological Land Classification Series (No. 24)*. Ottawa, ON and Montréal, QC: Sustainable Development Branch and Polyscience Publications Inc.

Neal, E. G., Hood, E., & Smikrud, K. (2010). Contribution of glacier runoff to freshwater discharge into the Gulf of Alaska. *Geophysical Research Letters*, *37*, L06404. https://doi.org/10.1029/2010GL042385

O'Donnell, J. A., Aiken, G. R., Butler, K. D., Guillemette, F., Podgorski, D. C., & Spencer, R. G. M. (2016). DOM composition and transformation in boreal forest soils: The effects of temperature and organic-horizon decomposition state. *Journal of Geophysical Research: Biogeosciences*, *121*(10), 2727–2744. https://doi.org/10.1002/2016JG003431

Oliver, A. A., Tank, S. E., Giesbrecht, I., Korver, M. C., Floyd, W. C., Sanborn, P., et al. (2017). A global hotspot for dissolved organic carbon in hypermaritime watersheds of coastal British Columbia. *Biogeosciences*, *14*(15), 3743–3762. https://doi.org/10.5194/bg-14-3743-2017

Pellerin, B. A., Saraceno, J. F., Shanley, J. B., Sebestyen, S. D., Aiken, G. R., Wollheim, W. M., & Bergamaschi, B. A. (2012). Taking the pulse of snowmelt: In situ sensors reveal seasonal, event and diurnal patterns of nitrate and dissolved organic matter variability in an upland forest stream. *Biogeochemistry*, *108*(1–3), 183–198. https://doi.org/10.1007/s10533-011-9589-8

Peralta-Tapia, A., Sponseller, R. A., Tetzlaff, D., Soulsby, C., & Laudon, H. (2015). Connecting precipitation inputs and soil flow pathways to stream water in contrasting boreal catchments. *Hydrological Processes*, *29*(16), 3546–3555. https://doi.org/10.1002/hyp.10300

Perdrial, J. N., McIntosh, J., Harpold, A., Brooks, P. D., Zapata-Rios, X., Ray, J., et al. (2014). Stream water carbon controls in seasonally snow-covered mountain catchments: Impact of inter-annual variability of water fluxes, catchment aspect and seasonal processes. *Biogeochemistry*, *118*(1–3), 273–290. https://doi.org/10.1007/s10533-013-9929-y

Peter, H., Singer, G. A., Preiler, C., Chifflard, P., Steniczka, G., & Battin, T. J. (2014). Scales and drivers of temporal $pCO_2$ dynamics in an Alpine stream. *Journal of Geophysical Research: Biogeosciences*, *119*(6), 1078–1091. https://doi.org/10.1002/2013JG002552

Raymond, P. A., McClelland, J. W., Holmes, R. M., Zhulidov, A. V., Mull, K., Peterson, B. J., et al. (2007). Flux and age of dissolved organic carbon exported to the Arctic Ocean: A carbon isotopic study of the five largest arctic rivers. *Global Biogeochemical Cycles*, *21*, GB4011. https://doi.org/10.1029/2007GB002934

Raymond, P. A., & Saiers, J. E. (2010). Event controlled DOC export from forested watersheds. *Biogeochemistry*, *100*(1–3), 197–209. https://doi.org/10.1007/s10533-010-9416-7

Raymond, P. A., Saiers, J. E., & Sobczak, W. V. (2016). Hydrological and biogeochemical controls on watershed dissolved organic matter transport: Pulse-shunt concept. *Ecology*, *97*(1), 5–16. https://doi.org/10.1890/14-1684.1

Salimon, C., dos Santos Sousa, E., Alin, S. R., Krusche, A. V., & Ballester, M. V. (2013). Seasonal variation in dissolved carbon concentrations and fluxes in the upper Purus River, southwestern Amazon. *Biogeochemistry*, *114*(1–3), 245–254. https://doi.org/10.1007/s10533-012-9806-0

Seifert, A. G., Roth, V. N., Dittmar, T., Gleixner, G., Breuer, L., Houska, T., & Marxsen, J. (2016). Comparing molecular composition of dissolved organic matter in soil and stream water: Influence of land use and chemical characteristics. *Science of the Total Environment*, *571*, 142–152. https://doi.org/10.1016/j.scitotenv.2016.07.033

Senar, O. E., Webster, K. L., & Creed, I. F. (2018). Catchment-scale shifts in the magnitude and partitioning of carbon export in response to changing hydrologic connectivity in a northern hardwood forest. *Journal of Geophysical Research: Biogeosciences*, *123*(8), 2337–2352. https://doi.org/10.1029/2018JG004468

Shanley, C. S., Pyare, S., Goldstein, M. I., Alaback, P. B., Albert, D. M., Beier, C. M., et al. (2015). Climate change implications in the northern coastal temperate rainforest of North America. *Climatic Change*, *130*(2), 155–170. https://doi.org/10.1007/s10584-015-1355-9

Shanley, J. B., Kendall, C., Smith, T. E., Wolock, D. M., & McDonnell, J. J. (2002). Controls on old and new water contributions to stream flow at some nested catchments in Vermont, USA. *Hydrological Processes*, *16*(3), 589–609. https://doi.org/10.1002/hyp.312

Shanley, J. B., Sebestyen, S. D., McDonnell, J. J., McGlynn, B. L., & Dunne, T. (2015). Water's Way at Sleepers River watershed—Revisiting flow generation in a post-glacial landscape, Vermont USA. *Hydrological Processes*, *29*(16), 3447–3459. https://doi.org/10.1002/hyp.10377

Smith, D. F., Podgorski, D. C., Rodgers, R. P., Blakney, G. T., & Hendrickson, C. L. (2018). 21 tesla FT-ICR mass spectrometer for ultrahigh-resolution analysis of complex organic mixtures. *Analytical Chemistry*, *90*(3), 2041–2047. https://doi.org/10.1021/acs.analchem.7b04159

Spencer, R. G. M., Kellerman, A. M., Podgorski, D. C., Macedo, M. N., Jankowski, K., Nunes, D., & Neill, C. (2019). Identifying the molecular signatures of agricultural expansion in Amazonian headwater streams. *Journal of Geophysical Research: Biogeosciences*, *124*(6), 1637–1650. https://doi.org/10.1029/2018JG004910

Spencer, R. G. M., Mann, P. J., Dittmar, T., Eglinton, T. I., McIntyre, C., Holmes, R. M., et al. (2015). Detecting the signature of permafrost thaw in Arctic rivers. *Geophysical Research Letters*, *42*(8), 2830–2835. https://doi.org/10.1002/2015GL063498

Stockinger, M. P., Bogena, H. R., Lücke, A., Diekkrüger, B., Cornelissen, T., & Vereecken, H. (2016). Tracer sampling frequency influences estimates of young water fraction and streamwater transit time distribution. *Journal of Hydrology*, *541*, 952–964. https://doi.org/10.1016/j.jhydrol.2016.08.007

Striegl, R. G., Dornblaser, M. M., Aiken, G. R., Wickland, K. P., & Raymond, P. A. (2007). Carbon export and cycling by the Yukon, Tanana, and Porcupine rivers, Alaska, 2001–2005. *Water Resources Research*, *43*. https://doi.org/10.1029/2006WR005201

Stubbins, A., & Dittmar, T. (2012). Low volume quantification of dissolved organic carbon and dissolved nitrogen. *Limnology and Oceanography: Methods*, *10*(5), 347–352. https://doi.org/10.4319/lom.2012.10.347

Stubbins, A., Lapierre, J. F., Berggren, M., Prairie, Y. T., Dittmar, T., & del Giorgio, P. A. (2014). What's in an EEM? Molecular signatures associated with dissolved organic fluorescence in boreal Canada. *Environmental Science & Technology*, *48*(18), 10598–10606. https://doi.org/10.1021/es502086e

Stubbins, A., Spencer, R. G. M., Chen, H., Hatcher, P. G., Mopper, K., Hernes, P. J., et al. (2010). Illuminated darkness: Molecular signatures of Congo River dissolved organic matter and its photochemical alteration as revealed by ultrahigh precision mass spectrometry. *Limnology and Oceanography*, *55*(4), 1467–1477. https://doi.org/10.4319/lo.2010.55.4.1467

Tank, S. E., Fellman, J. B., Hood, E., & Kritzberg, E. S. (2018). Beyond respiration: Controls on lateral carbon fluxes across the terrestrial-aquatic interface. *Limnology and Oceanography Letters*, *3*(3), 76–88. https://doi.org/10.1002/lol2.10065

Textor, S. R., Guillemette, F., Zito, P. A., & Spencer, R. G. M. (2018). An assessment of dissolved organic carbon biodegradability and priming in blackwater systems. *Journal of Geophysical Research: Biogeosciences*, *123*(9), 2998–3015. https://doi.org/10.1029/2018JG004470

Tiwari, T., Laudon, H., Beven, K., & Ågren, A. M. (2014). Downstream changes in DOC: Inferring contributions in the face of model uncertainties. *Water Resources Research*, *50*(1), 514–525. https://doi.org/10.1002/2013WR014275

Tomco, P. L., Zulueta, R. C., Miller, L. C., Zito, P. A., Campbell, R. W., & Welker, J. M. (2019). DOC export is exceeded by C fixation in May Creek: A late-successional watershed of the Copper River Basin, Alaska. *PLoS ONE*, *14*(11), e0225271. https://doi.org/10.1371/journal.pone.0225271

Tranvik, L. J., Downing, J. A., Cotner, J. B., Loiselle, S. A., Striegl, R. G., Ballatore, T. J., et al. (2009). Lakes and reservoirs as regulators of carbon cycling and climate. *Limnology and Oceanography*, *54*(6 part 2), 2298–2314. https://doi.org/10.4319/lo.2009.54.6_part_2.2298

Trumbore, S. (2006). Carbon respired by terrestrial ecosystems—Recent progress and challenges. *Global Change Biology*, *12*(2), 141–153. https://doi.org/10.1111/j.1365-2486.2006.01067.x

Vaughan, M. C. H., Bowden, W. B., Shanley, J. B., Vermilyea, A., & Schroth, A. W. (2019). Shining light on the storm: In-stream optics reveal hysteresis of dissolved organic matter character. *Biogeochemistry*, *143*(3), 275–291. https://doi.org/10.1007/s10533-019-00561-w

Wagner, S., Fair, J. H., Matt, S., Hosen, J. D., Raymond, P., Saiers, J., et al. (2019). Molecular hysteresis: Hydrologically driven changes in riverine dissolved organic matter chemistry during a storm event. *Journal of Geophysical Research: Biogeosciences*, *124*(4), 759–774. https://doi.org/10.1029/2018JG004817

Wang, T., Hamann, A., Spittlehouse, D. L., & Murdock, T. Q. (2012). Climate WNA: High resolution spatial climate data for western North America. *Journal of Applied Meteorology and Climatology*, *51*(1), 16–29. https://doi.org/10.1175/JAMC-D-11-043.1

Wiegner, T. N., Tubal, R. L., & MacKenzie, R. A. (2009). Bioavailability and export of dissolved organic matter from a tropical river during base- and stormflow conditions. *Limnology and Oceanography*, *54*(4), 1233–1242. https://doi.org/10.4319/lo.2009.54.4.1233

Wilson, H. F., Saiers, J. E., Raymond, P. A., & Sobczak, W. V. (2013). Hydrologic drivers and seasonality of dissolved organic carbon concentration, nitrogen content, bioavailability, and export in a forested New England stream. *Ecosystems*, *16*(4), 604–616. https://doi.org/10.1007/s10021-013-9635-6

Wilson, H. F., & Xenopoulos, M. A. (2009). Effects of agricultural land use on the composition of fluvial dissolved organic matter. *Nature Geoscience*, *2*(1), 37–41. https://doi.org/10.1038/ngeo391

Winterdahl, M., Wallin, M. B., Karlsen, R. H., Laudon, H., Öquist, M., & Lyon, S. W. (2016). Decoupling of carbon dioxide and dissolved organic carbon in boreal headwater streams. *Journal of Geophysical Research: Biogeosciences*, *121*(10), 2630–2651. https://doi.org/10.1002/2016JG003420

Worrall, F., Burt, T. P., Jaeban, R. Y., Warburton, J., & Shedden, R. (2002). Release of dissolved organic carbon from upland peat. *Hydrological Processes*, *16*(17), 3487–3504. https://doi.org/10.1002/hyp.1111

Worrall, F., Gibson, H. S., & Burt, T. P. (2008). Production vs. solubility in controlling runoff of DOC from peat soils—The use of an event analysis. *Journal of Hydrology*, *358*(1–2), 84–95. https://doi.org/10.1016/j.jhydrol.2008.05.037

Worrall, F., Burt, T., & Adamson, J. (2005). Fluxes of dissolved carbon dioxide and inorganic carbon from an upland peat catchment: Implications for soil respiration. *Biogeochemistry*, *73*(3), 515–539. https://doi.org/10.1007/s10533-004-1717-2

Zarnetske, J. P., Bouda, M., Abbott, B. W., Saiers, J., & Raymond, P. A. (2018). Generality of hydrologic transport limitation of watershed organic carbon flux across ecoregions of the United States. *Geophysical Research Letters*, *45*(21), 11,702–11,711. https://doi.org/10.1029/2018GL080005